Journal of Materials Chemistry C

Accepted Manuscript

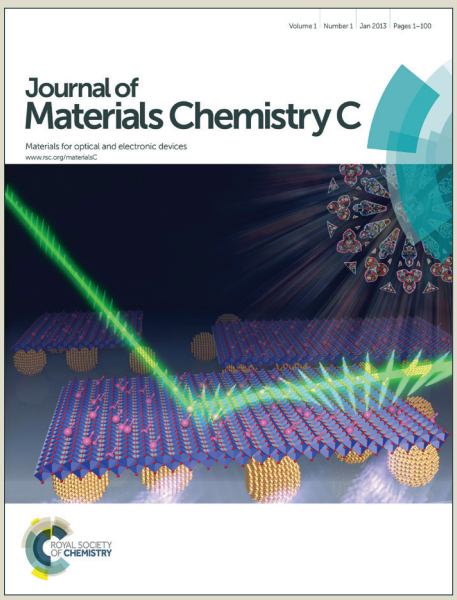

ROYAL SOCIETY OF CHEMISTRY

www.rsc.org/materialsC

Anomalous tunable visible to near infrared emission in Mn^{2+} doped spinel $MgGa_2O_4$ and room-temperature upconversion in the Mn^{2+} and Yb^{3+} codoped spinel

E. H. Song, J. L. Wang, D. C. Yu, S. Ye [a)] and Q. Y. Zhang [a)]

State Key Laboratory of Luminescent Materials and Devices, and Institute of Optical Communication Materials, South China University of Technology, Guangzhou 510641, China

Abstract

In contrast to common visible emission, an anomalous near-infrared (NIR) emission band at 790 nm has been demonstrated in spinel structure $MgGa_2O_4:Mn^{2+}$ with heavy Mn^{2+} doping. Tunable single-band visible to visible-NIR, and single-band NIR emission could be realized easily upon tuning the doping concentration of Mn^{2+}. Careful investigation on crystal structure, fluorescence lifetime and excitation & emission spectra indicates the NIR emission might be ascribed to the $^6A_1(^6S)^4T_1(^4G) \rightarrow {}^6A_1(^6S)^6A_1(^6S)$ transitions of the Mn^{2+}-Mn^{2+} dimers. When some Yb^{3+} ions are codoped into the spinel $MgGa_2O_4:Mn^{2+}$, room temperature visible upconversion (UC) emission can be realized upon excitation of a 976 nm laser diode. The temperature dependent UC emission properties as well as related UC mechanism have been investigated. Understanding the nature of Mn^{2+} Stokes and UC emission is the key to develop advanced photonic devices with improved properties and manufacturability for engineering applications.

Key words: Luminescence; Mn^{2+} ions; Near infrared; Spinel structure.

a) Author to whom correspondence should be addressed; Email: msyes@scut.edu.cn, qyzhang@scut.edu.cn

1. Introduction

In constant use since ancient times, luminescent materials activated by Mn^{2+} ions has become an indispensable and essential component in such fields as plasma display panels (PDP), field emission displays (FED), light emitting diodes (LEDs) owing to their unique properties including tunable excitation region but single-band emission with high chromaticity purity.[1-6] Due to the feature of *d-d* electronic transition, photoluminescence of Mn^{2+} is quite sensitive to crystal field strength of the substitute sites.[5] Thus, the photoluminescence of Mn^{2+} could be tuned from green to deep red feasibly upon Mn^{2+} located in different crystal field environments.[6-9] In contrast to the merits of Mn^{2+} tunable fluorescence, the spin-forbidden radiative transition [$^4T_1(^4G)\rightarrow{}^6A_1(^6S)$] of Mn^{2+} usually exhibits lower emission intensity, which significantly limits the application of Mn^{2+}-doped materials.[5] As an effective approach, increasing Mn^{2+} doping has been applied to improve the emission intensity of Mn^{2+}.[10, 11] However, it can be experimentally found that the emission intensity of Mn^{2+} is fast and greatly quenched with increasing the Mn^{2+}-doping concentration, due to strong exchange interaction between Mn^{2+}-Mn^{2+} pairs, especially in a host lattice with perovskite.[12, 13] Besides the concentration quenching among Mn^{2+} sub-lattices, the fast decrease of Mn^{2+} single-band emission in heavy Mn^{2+} doping might be induced by the introduction of other energy-dissipative channel additionally, like extra near-infrared (NIR) emission from the intermediate state.[12]

Here in this work, we report the realization of novel single-band NIR emission in $MgGa_2O_4$:Mn^{2+} using a heavy doping strategy. The underling mechanism of the anomalous NIR emission has been discussed based on the fluorescence lifetime and emission &

excitation spectra, and structure analysis. The Mn^{2+}-concentration and temperature-dependent NIR Stokes luminescence properties, along with the upconversion (UC) emission properties of Mn^{2+} in $MgGa_2O_4:Mn^{2+},Yb^{3+}$ have been investigated in details. A comprehensive understanding the nature of the Stokes and upconversion emission of Mn^{2+} is of fundamental importance for advancing technological applications.

2. Experimental

A series of $MgGa_2O_4:Mn^{2+},Yb^{3+}$ samples were synthesized by a high temperature solid state reaction method using MgO (99.99%), Ga_2O_3 (Analytically pure), Yb_2O_3 (99.998%) and $MnCO_3$ (99.95%) as raw materials. The Yb_2O_3 was purchased from Alfa Aesar Reagent Company and the others were supplied by Aladdin Industrial Corporation. The raw materials were weighed according to the nominal composition $Mg_{1-x}Mn_xGa_2O_4$ (x = 0-0.3) and $Mg_{1-x}Mn_xGa_{1.98}Yb_{0.02}O_4$ (x = 0-0.2), and then thoroughly milled. After that, the mixtures were sintered at 1350 ^{0}C for 4 hours under a weak reduction atmosphere (H_2/N_2 = 5/95). After being cooled down to room temperature naturally, the final products were obtained and reground them for further characterization.

The crystal structure of the samples are characterized by a Rigaku D/max-IIIA x-ray diffractometer with Cu-Kα radiation (λ = 1.5418 Å). The emission and excitation spectra, as well as decay curves were recorded by a fluorescence spectrometer (FLS 920, Edinburgh Instruments). The UC emission spectra were recorded on a TRIAX320 fluorescence spectrofluorometer (Jobin-Yvon Co., France) equipped with a R928 photomultiplier tube (PMT) upon continuous wave excitation of a 976 nm Laser Diode (LD) (Coherent corp.,

USA). To study thermal quenching of the UC luminescence, the spectrofluorimeter was equipped with a TAP-02 High- temperature fluorescence instrument (Tian Jin Orient – KOJI instrument Co., Ltd.).

3. Results and discussions

XRD patterns of the as-prepared samples generally confirmed the presence of $MgGa_2O_4$:Mn^{2+} (ICSD card no 411206) as sole crystalline phase as shown in **Fig. 1.** The compound $MgGa_2O_4$ belongs to the cubic spinel structure with F*d-3m* space group (no. 227) and the lattice constants are $a = b = c = 8.288$ Å. In this structure, both Mg^{2+} and Ga^{3+} ions simultaneously occupy the 8a and 16d crystallographic positions (Wyckoff notation). When some Mn^{2+} ions are doped into $MgGa_2O_4$, they would simultaneously substitute for both tetrahedral and octahedral Mg^{2+} ions due to their same valence state and similar ion radii (Coordination number (CN) = 4, r = 0.66 Å for Mn^{2+} and r = 0.57 Å for Mg^{2+}; CN = 6, r = 0.80 Å for Mn^{2+} and r = 0.72 Å for Mg^{2+}).[14]

Fig. 2(a) shows the emission spectra of $Mg_{1-x}Mn_xGa_2O_4$ (x = 0.01-0.30) under 300 nm UV light excitation. For the samples with lower Mn^{2+} (x = 0.01-0.05) doping concentration, the emission spectra consist of a pure visible (VIS) emission band centered at 507 nm, which corresponds to the $^4T_1(^4G)\rightarrow{}^6A_1(^6S)$ transitions of tetrahedral Mn^{2+} ions.[15] Interestingly, when the doping concentration of Mn^{2+} increases to heavy enough (x = 0.10-0.20), an extra near infrared (NIR) emission band at approximately 791 nm appears in the emission spectra besides the VIS emission. More importantly, as the doping concentration of Mn^{2+} further reaches at x = 0.30, the VIS emission is fully quenched, a pure NIR (791 nm) mission band

was realized, which indicates that the concentration quenching effect of VIS emission is more serious than that of NIR emission. The VIS and NIR emission show a maximum intensity at x = 0.02 and 0.20, respectively. These phenomena also demonstrate that the energy absorbed by Mn^{2+} ions can be converted into NIR emission, resulting in the Mn^{2+} visible emission fast quenched. To get more insights about the interesting NIR emission, luminescence decay curves of both NIR and VIS emissions in $Mg_{1-x}Mn_xGa_2O_4$ were measured under 300 nm UV light excitation, shown in **Fig. 2**. The fluorescence lifetime of both emission bands decrease monotonously with the increase of Mn^{2+} doping concentration. For NIR emission, luminescence decay curves in **Fig. 2(b)** exhibit obvious deviation from the single-exponential decay, which clearly reveals that muitiple processes may be involved in the decay of the NIR emission besides the radiative transition. The mean decay lifetime (τ_m) is given by $\tau_m = \int_{t_0}^{\infty} [I(t)/I_0]dt$, where I(t) is the luminescence intensity as a function of time t and I_0 represents the maximum of I(t) which occurs at the initial time t_0. It is determined that the fluorescence lifetime of NIR emission is between 4.290 and 1.340 ms. Meanwhile, the VIS emission exhibits the near single-exponential decay behavior for lower Mn^{2+} concentration (x = 0.01 and 0.02), and the lifetimes are calculated to be 3.822 and 3.150 ms for x = 0.01 and 0.02, respectively. As the doping concentration of Mn^{2+} further rises to high enough (x = 0.05-0.20), the fluorescence decay curves exhibit external non single-exponential decay behavior. The fluorescence lifetime is sharply shortening from 1.484 to 0.010 ms with the increases x = 0.05 to 0.20 due to the increasing nonradiative loss processes among Mn^{2+} ions. These significant different emission behaviors clearly demonstrate that the VIS and NIR emission bands originate from two different emission centers.

As shown in **Fig. 2(a)**, with the increases Mn^{2+} content (x) from x = 0.01 to 0.20, the emission wavelength of VIS emission band monotonously shifted from 507 to 518 nm while the emission wavelength of NIR emission showed no shift in the whole range, which might be ascribed to the changed or unaffected coordination environment of the two emission centers.[15] Therefore, to explore the physical origin of the NIR emission band, excitation spectra of both $Mg_{0.99}Mn_{0.01}Ga_2O_4$ (monitored at 507 nm) and $Mg_{0.8}Mn_{0.2}Ga_2O_4$ (monitored at 518, and 791 nm) were detected and given in **Fig. 3**. The excitation spectrum in **Fig. 3(a)** (monitored at 507 nm) is composed of a broad band located around 280 nm and several typical sharp excitation bands located between 350 to 500 nm, which can be attributed to the charge transfer band (CTB) of Mn^{2+}-O^{2-} and spin-forbidden d-d transitions of Mn^{2+} ions, respectively.[16] The bands at 380, 425, 445 and 480 nm are corresponded to the transitions of tetrahedral Mn^{2+} from the ground state $^6A_1(^6S)$ to the $^4T_2(^4D)$, $[^4A_1(^4G),^4E(^4G)]$, $^4T_2(G)$ and $^4T_1(G)$ energy levels, respectively.[16] Further monitoring the emission wavelengths of 518 and 791 nm, two similar excitation spectra are obtained (**Fig. 3(b)**), implying that both the VIS and NIR emission bands in this system originated from the tetrahedral Mn^{2+} ions. Generally, the tetrahedrally coordinated (weak crystal field) Mn^{2+} ions give green emission and the octahedral coordinated (strong crystal field) Mn^{2+} ions exhibit orange to red emission.[5] Herein, the contribution from the crystal-field change can be ruled out because blue shifted emission is expected when Mg^{2+} ions are replaced by larger Mn^{2+} ions. Although, Mn^{2+} ions would simultaneously occupy both the tetrahedral and octahedral Mg^{2+} sites in $MgGa_2O_4$, the NIR emission cannot be attributed to octahedral Mn^{2+} ions since Mn^{2+} would show red emission (at 674 nm) in octahedral sites for this system.[17] Therefore, the NIR

emission band in $MgGa_2O_4:Mn^{2+}$ should be attributed to other mechanism.

Compared to the f-shells of lanthanide ions, the d-shells of Mn^{2+} ions are not fully isolated from their environment, especially, when Mn^{2+} ions are close enough (several angstroms) in a host lattice they can form Mn^{2+}-Mn^{2+} dimers via superexchange interactions.[13, 18, 19] For spinel structure $MgGa_2O_4$, the tetrahedral MgO_4 and octahedral MgO_6 are connected to each other by sharing an oxygen atom corner and the nearest distance between tetrahedral Mg^{2+} and octahedral Mg^{2+} is 3.436 Å (ICSD 411206). Since Mn^{2+} can substitute for tetrahedral and octahedral Mg^{2+} in this structure, it has a great chance to form the Mn^{2+}-Mn^{2+} dimers of tetrahedral Mn^{2+} (Mg^{2+})-O^{2-}-octahedral Mn^{2+}(Mg^{2+}) in $MgGa_2O_4:Mn^{2+}$. Notably, the Mn^{2+}-Mn^{2+} dimers can also act as the emission centers in a suitable host lattice, and providing a longer emission wavelength band than that of the isolated Mn^{2+} ion due to the change of energy gap between ground and excited states.[13, 20] However, the broad emission bands of isolated Mn^{2+} ions and Mn^{2+}-Mn^{2+} dimers usually have a large overlap and cannot be spectrally resolved.[15, 19] With increasing Mn^{2+} concentration, more Mn^{2+}-Mn^{2+} dimers will be formed, which is in good agreement with above results of the observation of ratio between the emission intensities of the two emission bands (VIS and NIR) with increasing Mn^{2+} concentration in $Mg_{1-x}Ga_2O_4:xMn^{2+}$. Therefore, it is concluded that the NIR emission originates from the $^6A_1(^6S)^4T_1(^4G) \rightarrow {}^6A_1(^6S)^6A_1(^6S)$ transitions of Mn^{2+}-Mn^{2+} dimers. [12, 13]

To further compare the difference of the VIS and NIR emission bands, **Fig. 4(a)** gives the emission spectra of $Mg_{0.8}Mn_{0.2}Ga_2O_4$ at various temperatures (50-300 K) under 300 nm UV light excitation. With increasing temperature, the two emission bands show a significant different thermal quenching behavior. The VIS emission exhibits a monotonous-decrease

trend in the whole temperature range. While, the NIR emission shows a slight increase with increases the temperature from 50 to 100 K, and then gradually decrease with further increasing the temperature. **Fig. 4(b)** clearly shows the emission intensity of the two emission bands as a function of temperature. It can be observed that when the temperature rises to 100 K, the emission intensity of the VIS emission sharply decreased to 16.7% of its initial intensity. As the temperature is further increased to 300 K, only 1.3% of its initial intensity can be remained. Meanwhile, the emission intensity of the NIR emission exhibits 108% and 18.7% of its initial value at 100 and 300 K, respectively. This fact indicates that the thermal quenching of VIS emission (from isolated Mn^{2+} ions) is more serious than that of NIR emission (from Mn^{2+}-Mn^{2+} pairs) in this structure.

We also attempted to introduce some Yb^{3+} ions into $Mg_{1-x}Mn_xGa_2O_4$ (x = 0.01-0.20) to explore the possibility of generating UC luminescence for the two emission bands. **Figure 5(a)** shows the UC emission spectra of $Mg_{1-x}Mn_xGa_{1.98}Yb_{0.02}O_4$ (x = 0.01-0.20) under the excitation of a 976 nm LD. It can be observed that all emission spectra consist of a visible emission band centered at ~507 nm, which are consistent well with the visible emission shown in **Fig. 2(a)**, indicating visible UC emission of Mn^{2+} has been realized in this system. While, the NIR (791 nm) UC emission has not been achieved. With the increase Mn^{2+} content, the UC emission intensity of the visible emission gradually increases and gets the maximum at x = 0.05, and then sharply decreased with further increasing Mn^{2+} content because of the concentration quenching effect.[21] As doping concentration of Mn^{2+} reaches at x = 0.2, the visible UC emission is thoroughly quenched, implying that the concentration quenching effect in UC emission is more serious than that of stokes emission.

To further understanding the visible UC behavior, the power dependence of the integrated UC emission intensity on a log–log scale for $Mg_{0.95}Mn_{0.05}Ga_{1.98}Yb_{0.02}O_4$ is shown in **Fig. 5(b)**, the slope is 1.59, which firmly reveals that the visible UC emission of Mn^{2+} belongs to a two-photon process.[22] The result matches well with the excitation from the ground state $^6A_1(^6S)$ to the excited state $^4T_1(^4G)$ in Mn^{2+} due to the energy gap is about 2.53 eV and two 976 nm (1.27 eV) photons are theoretically required in the UC processes. Since the cooperative UC emission band of Yb^{3+} has not been obtained either in $Mg_{1-x}Mn_xGa_{1.98}Yb_{0.02}O_4$ or $MgGa_{1.98}Yb_{0.02}O_4$, the cooperative sensitive UC emission mechanism in this system could be ruled out, the visible UC emission here should be ascribed to the Yb^{3+} and Mn^{2+} ions formed some unique UC emission centers (Yb^{3+}-Mn^{2+} dimers).

To explore the UC emission mechanism in $MgGa_2O_4:Mn^{2+},Yb^{3+}$, the crystal structure of $MgGa_2O_4$ and the $Mn^{2+}(Yb^{3+})$ ions occupied sites are further analyzed. Based on the analysis above, it can be known that the compound $MgGa_2O_4$ belongs to a typical spinel structure, in this structure, both Mg^{2+} and Ga^{3+} ions simultaneously occupy the 8a and 16d crystallographic positions (Wyckoff notation) (ICSD 411206). When some Yb^{3+} and Mn^{2+} ions are codoped into the spinel structure $MgGa_2O_4$, they would replace both Ga^{3+} and Mg^{2+} ions based on the consideration of ionic radius and valence state. Therefore the tetrahedrally coordinated $Yb^{3+}(Mn^{2+})$ and octahedrally coordinated $Yb^{3+}(Mn^{2+})$ can be formed theoretically in $MgGa_2O_4:Mn^{2+},Yb^{3+}$. Meanwhile, the shortest distance between octahedral Ga^{3+} and tetrahedral Mg^{2+} is about 3.436 Å, and the GaO_6 octahedron and MgO_4 tetrahedron are linked each other by sharing with an oxygen atom with a connectivity angle$\angle Ga^{3+}$-O^{2-}-Mg^{2+} of around 123^o (ICSD 411026). In addition, the green and NIR emission bands in this system are

attributed to the tetrahedrally coordinated Mn^{2+} and tetrahedral Mn^{2+}-octaheral Mn^{2+} dimers, respectively. Therefore, it can be deduced that the exchange coupled Yb^{3+}(octahedral Ga^{3+})-Mn^{2+}(tetrahedral Mg^{2+}) pair has the possibility to form in Yb^{3+}-Mn^{2+} codoped $MgGa_2O_4$. Because of the exchange interactions between Yb^{3+} and Mn^{2+}, the emission of Yb^{3+}can be obtained by excitation Mn^{2+} (down conversion) and the Mn^{2+} emission can be realized by excitation Yb^{3+} (UC) in a suitable host.[12, 23, 24] Based on these facts, the ground state absorption (GSA) and excited state absorption (ESA) UC mechanism based on Yb^{3+}-Mn^{2+} pair is proposed to explain the visible UC emission, shown in **Fig. 5(c)**. The GSA step excites the pair from the $\left|{}^2F_{7/2}, {}^6A_1({}^6S)\right\rangle$ ground state into the $\left|{}^2F_{5/2}, {}^6A_1({}^6S)\right\rangle$ intermediate excited state, which is mainly localized on the Yb^{3+} ion. In the ESA step, the pair is further promoted from $\left|{}^2F_{5/2}, {}^6A_1({}^6S)\right\rangle$ state into the $\left|{}^2F_{7/2}, {}^4T_1({}^4G)\right\rangle$ emitting state, and then emits a visible photon. [25] The detail luminescence processes are shown as follows:

$$\left|{}^2F_{7/2}, {}^6A_1({}^6S)\right\rangle + h\nu\ (976\ nm) \rightarrow \left|{}^2F_{5/2}, {}^6A_1({}^6S)\right\rangle \quad (GSA)$$

$$\left|{}^2F_{5/2}, {}^6A_1({}^6S)\right\rangle + h\nu\ (976\ nm) \rightarrow \left|{}^2F_{7/2}, {}^4T_1({}^4G)\right\rangle \quad (ESA)$$

$$\left|{}^2F_{7/2}, {}^4T_1({}^4G)\right\rangle \rightarrow \left|{}^2F_{7/2}, {}^6A_1({}^6S)\right\rangle + h\nu\ (\sim 507\ nm)$$

Owing to the isolated Mn^{2+} ions and Mn^{2+}-Mn^{2+} dimers have no absorption around 980 nm, both of them show no UC emission upon excitation of a 976 nm- LD for Mn^{2+} ions solely doped $MgGa_2O_4$, which can be obtained only in Yb^{3+}/Mn^{2+}codoped system. However, in $MgGa_2O_4$:Mn^{2+},Yb^{3+}, the visible emission can be realized, the NIR emission band (centered at 791 nm) cannot be. On the other hand, the cooperative sensitization mechanism for Mn^{2+} has been excluded. Accordingly, the visible UC emission in $MgGa_2O_4$:Mn^{2+},Yb^{3+} is ascribed to the Yb^{3+}-Mn^{2+} pairs formed by Yb^{3+} and isolated Mn^{2+} ions through exchange interaction.

However, it is difficult to form the unique UC emission centers of Yb^{3+}-Mn^{2+}-Mn^{2+} clusters through exchange interaction between Mn^{2+}-Mn^{2+} dimers and Yb^{3+} ions because the exchange interactions in Mn^{2+}-Mn^{2+} dimers and Mn^{2+}-Yb^{3+} pairs are simultaneously existence. In theory, the two exchange interactions compete with each other, leading to difficultly balancing them. Therefore, when the exchange interaction in Mn^{2+}-Mn^{2+} dimers is much weaker than that of Yb^{3+}-Mn^{2+} pairs, the Yb^{3+}-Mn^{2+}-Mn^{2+} cluster will decompose into Yb^{3+}-Mn^{2+} dimer, thus the NIR emission cannot be obtained.

Thermal stability is an important parameter not only for practical application but also for fundamental research. Moreover, the previous reported Yb^{3+}/Mn^{2+} codoped UC luminescence systems usually show efficient UC luminescence only below 100 K.[26-28] Thereby the dependence of UC luminescence on temperature was investigated here. **Fig. 5(d)** displays the UC emission spectra of $Mg_{0.95}Mn_{0.05}Ga_{1.98}Yb_{0.02}O_4$ at various temperatures from 300 to 473 K upon excitation of a 976 nm LD. It can be observed that all UC emission spectra are composed of a broad band between 450 and 600 nm with a maximum at ~507 nm, originating from the $\left|{}^2F_{7/2}, {}^4T_1({}^4G)\right\rangle \rightarrow \left|{}^2F_{7/2}, {}^6A_1({}^6S)\right\rangle$ transitions of Yb^{3+}-Mn^{2+} pairs. As the temperature increases, the band shape and peak position show little changes while the UC emission intensity decreased greatly due to the serious nonradiative transition loss processes. Notably, the green UC emission can be seen by naked eyes even when the temperature increases to 473 K, showing good thermal stability and which may be applied in practice. For UC emission of Yb^{3+}-Mn^{2+} pairs, the nonradiative transition loss processes are mainly ascribed to the multi-phonon relaxation processes from $\left|{}^2F_{7/2}, {}^4T_1({}^4G)\right\rangle$ to $\left|{}^2F_{7/2}, {}^4T_1({}^4G)\right\rangle$, therefore the larger energy gap between $\left|{}^2F_{7/2}, {}^4T_1({}^4G)\right\rangle$ and

$\left|{}^2F_{7/2}, {}^4T_1({}^4G)\right\rangle$ would result in the slighter multi-phonon relaxation processes.[23, 29] Compared with previous Yb^{3+}-Mn^{2+} codoped UC systems reported by H. U. Güdel and coworkers[2], the energy gap between $\left|{}^2F_{7/2}, {}^4T_1({}^4G)\right\rangle$ and $\left|{}^2F_{7/2}, {}^4T_1({}^4G)\right\rangle$ in $MgGa_2O_4$:Yb^{3+},Mn^{2+} is much larger which may be the main reason for its good thermal stability.

4. Conclusions

In summary, an anomalous NIR emission band centered at 790 nm has been demonstrated in $MgGa_2O_4$:Mn^{2+} in additional to the conventional green emission. Upon varying the doping concentration of Mn^{2+}, single band visible emission to single band NIR emission can be realized easily. The visible UC emission can be obtained while the NIR UC cannot be in Yb^{3+}/Mn^{2+} codoped $MgGa_2O_4$. Crystal structure analysis, emission & excitation spectra and fluorescence lifetime analysis demonstrated that the NIR emission originates from the $^6A_1(^6S)^4T_1(^4G) \rightarrow {}^6A_1(^6S)^6A_1(^6S)$ transitions of Mn^{2+}-Mn^{2+} dimers, while the visible emission is attributed from the $^4T_1(^4G) \rightarrow {}^6A_1(^6S)$ transitions of the isolated Mn^{2+} ions. The UC mechanism of the visible emission can be ascribed to the GSA/ESA UC mechanism. The present work provides new insights about Mn^{2+} emission, which is of importance in efficient optoelectronic devices.

Acknowledgments

This work is financially supported by NSFC (Grant Nos. 51125005, 21101065 and U0934001), and China Postdoctoral Science Foundation funded project (2012M511558).

References:

1. R. Beaulac, P. I. Archer, S. T. Ochsenbein and D. R. Gamelin, *Adv. Funct. Mater.*, 2008, **18**, 3873.
2. J. F. Suyver, A. Aebischer, D. Biner, P. Gerner, J. Grimm, S. Heer, K. W. Krämer, C. Reinhard and H. U. Güdel, *Opt. Mater.*, 2005, **27**, 1111.
3. X. J. Wang, R. J. Xie, D. Benjamin, T. Takeda, T. Suehiro, N. Hirosaki, T. Sekiguchi, H. L. Li and Z. Sun, *Dalton Trans.*, 2014, **43**, 6120.
4. J. H. Yu, S. Kwon, Z. Petrášek, O. K. Park, S. W. Jun, K. Shin, M. Choi, Y. I. Park, K. Park, H. B. Na, N. Lee, D. W. Lee, J. H. Kim, P. Schwille and T. Hyeon,, *Nature Mater.*, 2013, **12**, 359.
5. G. Blasse and B. C. Grabmaier, *Luminescent materials*, Vol. 44 (Springer, 1994).
6. S. Ye, F. Xiao, Y. X. Pan, Y. Y. Ma and Q. Y. Zhang, *Mater. Sci. Eng. Rep*., 2010, **71**, 1.
7. X. Chen, P. P. Dai, X. T. Zhang, C. Li, S. Lu, X. L. Wang, Y. Jia and Y. C. Liu, *Inorg. Chem.*, 2014, **53**, 3441.
8. T. S. Chan, R. S. Liu and I. Baginskiy, *Chem. Mater.*, 2008, **20**, 1215.
9. H. Lin, R. Zhang, D. Q. Chen, Y. L. Yu, A. P. Yang and Y. S. Wang, *J. Mater. Chem. C*, 2013, **1**, 1804.
10. J. Lü, F. P. Du, R. Zhu, Y. L. Huang and H. J. Seo, *J. Mater. Chem.*, 2011, **21**, 16398.
11. J. Lin, Q. Zhang, L. Wang, X. C. Liu, W. B. Yan, T. Wu, X. H. Bu and P. Y. Feng, *J. Am. Chem. Soc.*, 2014, **136**, 4769.
12. E. H. Song, S. Ding, M. Wu, S. Ye, F. Xiao, S. F. Zhou and Q. Y. Zhang, *Adv. Opt. Mater.*, 2014, **2**, 670.
13. A. P. Vink, M. A. De Bruin, S. Roke, P. S. Peijzel and A. Meijerink, *J. Electrochem. Soc.*, 2001, **148**, E313.
14. R. D. Shannon, *Acta Crystallogr., Sec. A: Cryst. Phys., Diffr., Theor. Gen. Crystallogr.*, 1976, **32**, 751.
15. L. Shi, Y. L. Huang and H. J. Seo, *J. Phys. Chem. A*, 2010, **114**, 6927.
16. H. Matsui, C. N. Xu, M. Akiyama and T. Watanabe, *Jpn. J. Appl. Phys.,* 2000, **39**, 6582.
17. H. Kudo, M. Kitaya, H. Kobayashi, M. Shirai, K. Tanaka, Y. Kawabe and E. Hanamura, *J. Phys. Soc. Jpn.*, 2006, **75**, 14701.

18. C. Barthou, J. Benoit, P. Benalloul and A. Morell, *J. Electrochem. Soc.*, 1994, **141**, 524.

19. C. R. Ronda and T. Amrein, *J. Lumin.*, 1996, **69**, 245.

20. C. Kulshreshtha, J. H. Kwak, Y. Park and K. Sohn, *Opt. Lett.*, 2009, **34**, 794.

21. C. Reinhard, R. Valiente and H. U. Güdel, *J. Phys. Chem. B*, 2002, **106**, 10051.

22. M. Pollnau, D. R. Gamelin, S. R. Lüthi, H. U. Güdel and M. P. Hehlen, *Phys. Rev. B: Condens. Matter*, 2000, **61**, 3337.

23. E. H. Song, S. Ding, M. Wu, S. Ye, F. Xiao, G. P. Dong and Q. Y. Zhang, *J. Mater. Chem. C*, 2013, **1**, 4209.

24. G. J. Gao and L. Wondraczek, *J. Mater. Chem. C*, 2013, **1**, 1952.

25. P. Gerner, C. Reinhard and H. U. Güdel, *Chem-Eur. J.*, 2004, **10**, 4735.

26. R. Martín-Rodríguez, R. Valiente and M. Bettinelli, *Appl. Phys. Lett.*, 2009, **95**, 91913.

27. S. Ye, Y. J. Li, D. C. Yu, G. P. Dong and Q. Y. Zhang, *J. Mater. Chem.*, 2011, **21**, 3735.

28. E. H. Song, S. Ding, M. Wu, S. Ye, Z. T. Chen, Y. Y. Ma and Q. Y. Zhang, *Opt. Mater. Express*, 2014, **4**, 1186.

29. P. Gerner, C. Fuhrer, C. Reinhard and H. U. Güdel, *J. Alloy. Compd.*, 2004, **380**, 39.

Figure captions

Fig. 1. XRD Pattern of $Mg_{0.7}Mn_{0.3}Ga_2O_4$. A standard diffraction pattern of $MgGa_2O_4$ (ICSD card no 411206) is included for comparison.

Fig. 2. Emission spectra (a), and corresponding luminescence decay curves (b and c) of $Mg_{1-x}Mn_xGa_2O_4$ upon 300 nm UV light excitation.

Fig. 3. Excitation spectra of $Mg_{0.99}Mn_{0.01}Ga_2O_4$ (a), and $Mg_{0.8}Mn_{0.2}Ga_2O_4$ (b).

Fig. 4. Temperature-dependent emission spectra (a), and corresponding emission intensity of $Mg_{0.8}Mn_{0.2}Ga_2O_4$ (b) under 300 nm UV light excitation.

Fig. 5. Room temperature UC emission spectra of $Mg_{1-x}Mn_xGa_{1.98}Yb_{0.02}O_4$ upon excitation of a 976 nm LD (a), Log-log plots of the UC emission intensity versus pump power of Mn^{2+} in $Mg_{0.95}Mn_{0.05}Ga_{1.98}Yb_{0.02}O_4$ (b), Proposed UC mechanism in $Mg_{1-x}Mn_xGa_{1.98}Yb_{0.02}O_4$ (c), and UC emission spectra of $Mg_{0.95}Mn_{0.05}Ga_{1.98}Yb_{0.02}O_4$ as a function of temperature under the excitation of a 976 nm LD (d).

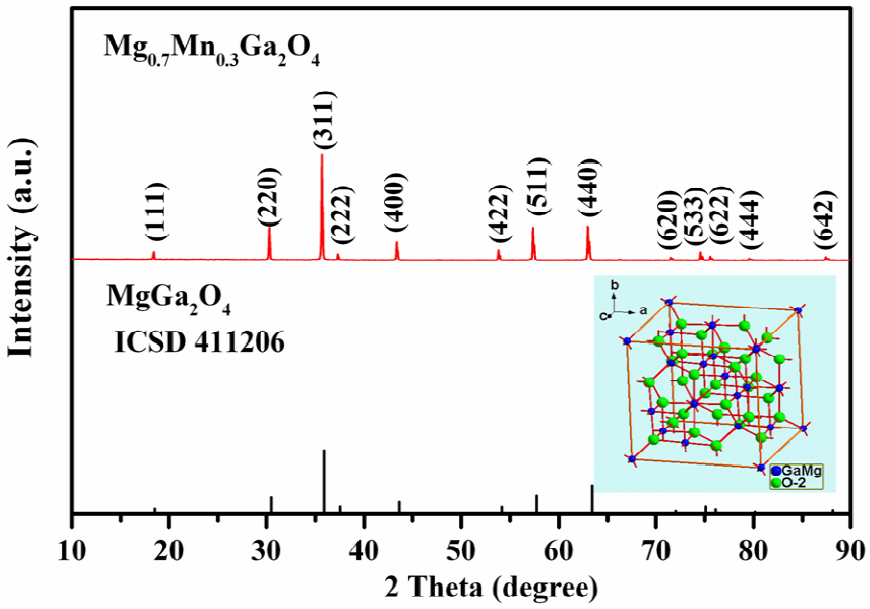

Fig. 1

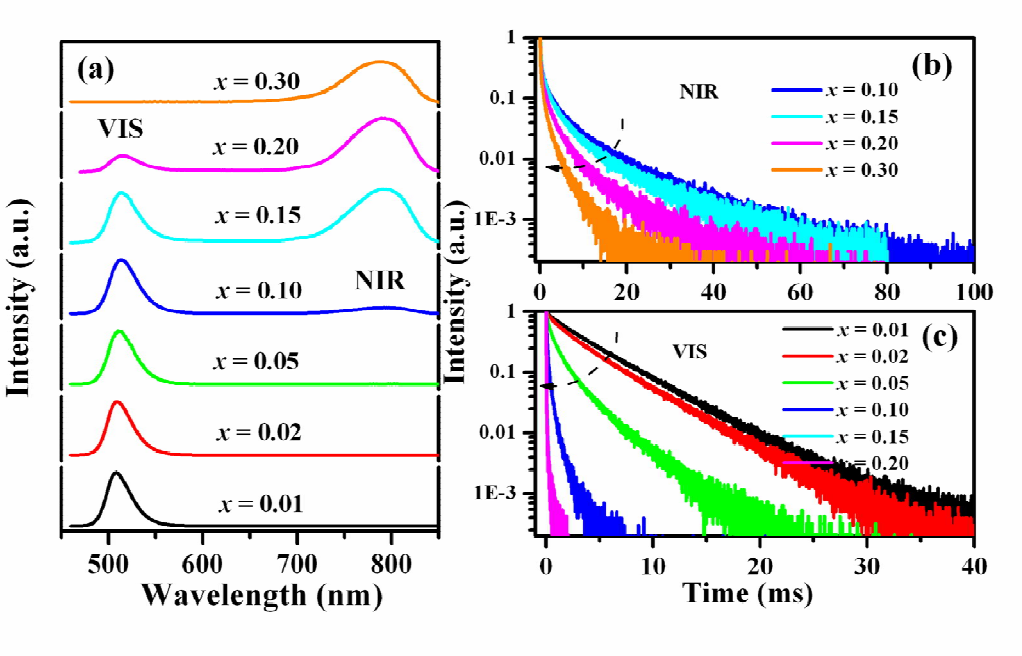

Fig. 2

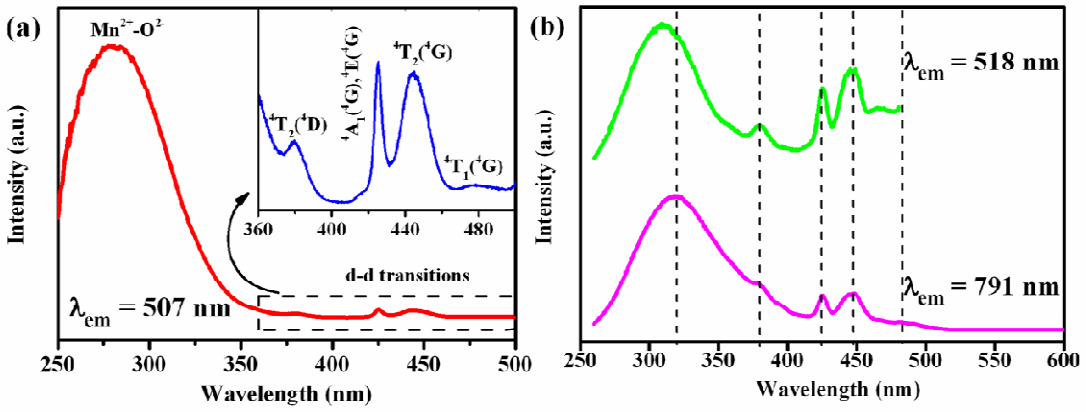

Fig. 3

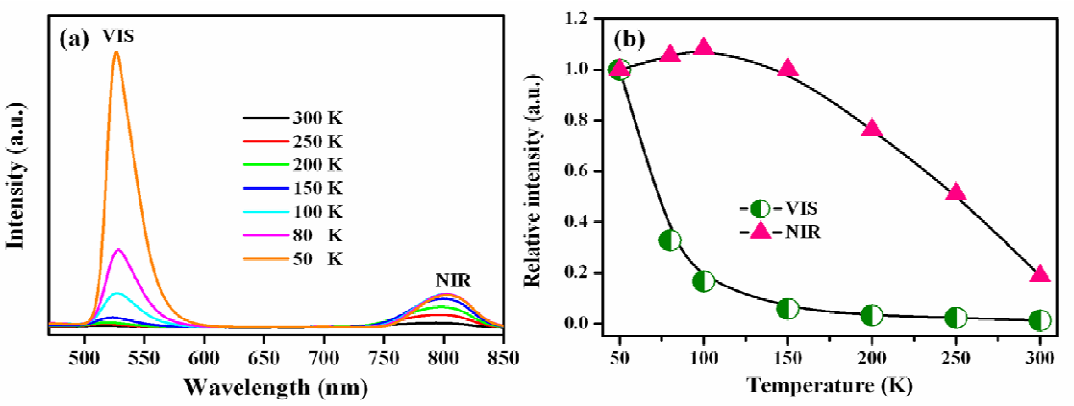

Fig. 4

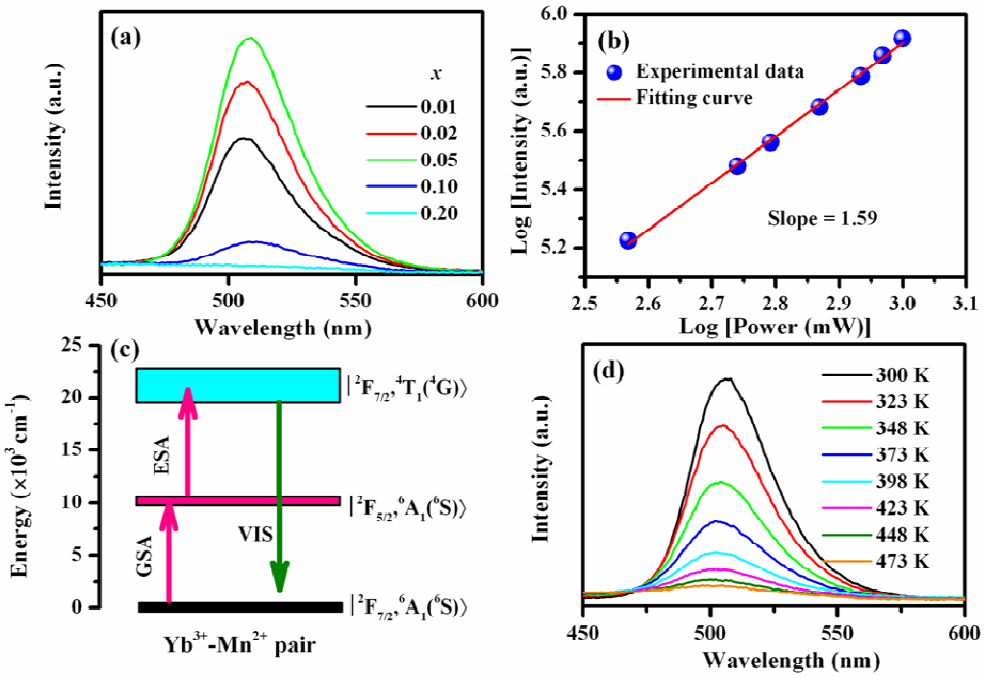

Fig. 5

Graphical abstract:

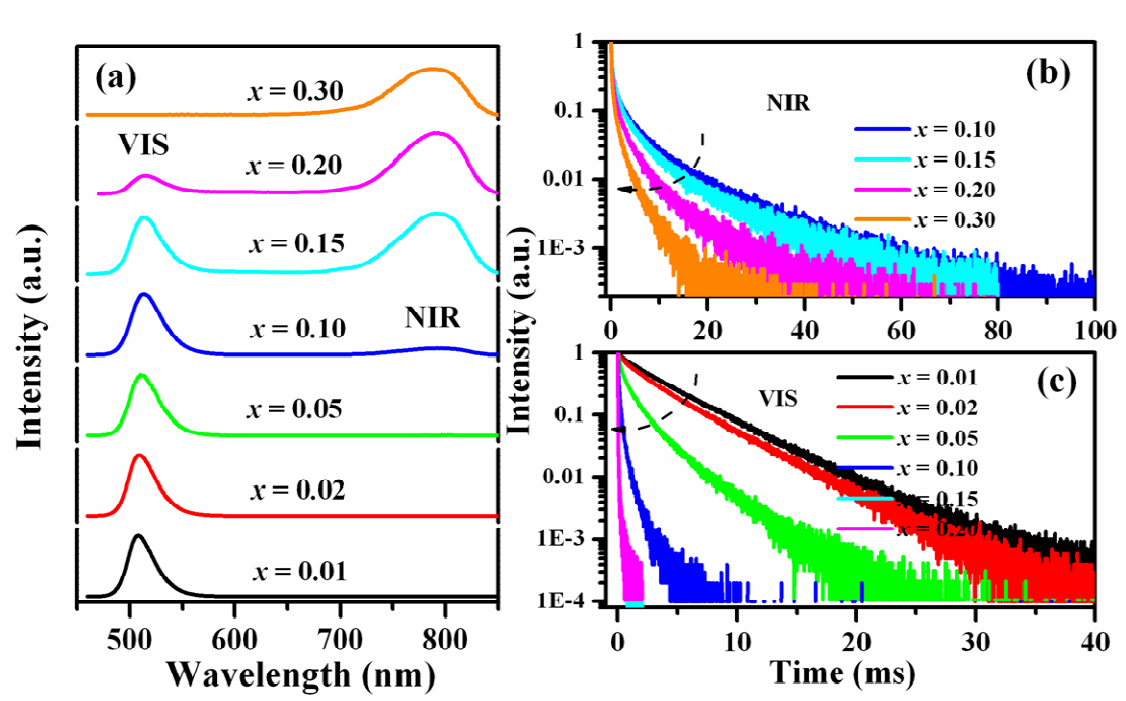

In contrast to common visible emission, an anomalous near-infrared emission at 790 nm has been demonstrated in spinel structure $MgGa_2O_4:Mn^{2+}$ with heavy Mn^{2+} doping.